

Bouncing ball dynamics: simple model of motion of the table and sinusoidal motion

Andrzej Okniński¹⁾, Bogusław Radziszewski²⁾
Kielce University of Technology, 25-314 Kielce, Poland¹⁾
Collegium Mazovia Innovative University, 08-110 Siedlce, Poland²⁾

October 30, 2018

Abstract

Nonlinear dynamics of a bouncing ball moving vertically in a gravitational field and colliding with a moving limiter is considered and the Poincaré map, describing evolution from an impact to the next impact, is described. Displacement of the table is approximated in one period by four cubic polynomials. Results obtained for this model are used to elucidate dynamics of the standard model of bouncing ball with sinusoidal motion of the limiter.

1 Introduction

In the present paper we study dynamics of a small ball moving vertically in a gravitational field and impacting with a periodically moving limiter (a table). This model belongs to the field of nonsmooth and nonlinear dynamical systems [1, 2, 3, 4]. In such systems nonstandard bifurcations such as border-collisions and grazing impacts leading often to complex chaotic motions are typically present. It is important that nonsmooth systems have many applications in technology [5, 6, 7, 8, 9].

Impacting systems studied in the literature can be divided into three main classes: bouncing ball models [10, 11, 12], impacting oscillators [13] and impacting pendulums [14, 9], see also [1]. In dynamics with impacts it is usually difficult or even impossible to solve nonlinear equation for an instant of the next impact. For example, in the bouncing ball models the table's motion has been usually assumed in sinusoidal form, cf. [12] and references therein. This choice of the limiter's motion leads indeed to nontractable nonlinear equation for time of the next impact. To tackle this problem we proposed a sequence of models in which periodic motion of the table is assumed (in one period of limiter's motion) as a low-order polynomial of time [15]. It is thus possible to approximate the sinusoidal motion of the table more and more exactly and conduct analytical computations. Carrying out this plan we have studied several such models with linear, quadratic and cubic polynomials [16, 17, 18, 19].

In the present work we conduct analytical and numerical investigations of the model in which sinusoidal displacement of the table is approximated in one period by four cubic polynomials. We shall refer to this model as \mathcal{M}_C . Simultaneously, we study the standard dynamics of bouncing ball with sinusoidal motion of the limiter, referred to as \mathcal{M}_S . We hope that rigorous results obtained for the model \mathcal{M}_C cast light on dynamics of \mathcal{M}_S . It should be stressed that results obtained for the model \mathcal{M}_S can be compared with experimental studies, see [20, 21, 22] for the early papers, summarized in [23], and [24] for recent work.

The paper is organized as follows. In Section 2 a one dimensional dynamics of a ball moving in a gravitational field and colliding with a table is reviewed and the corresponding Poincaré map is constructed and models of the limiter's motion \mathcal{M}_C and \mathcal{M}_S are defined. Bifurcation diagrams are computed for \mathcal{M}_C and \mathcal{M}_S . In Sections 3, 4 and 5 a combination of analytical and numerical approach is used to investigate selected problems of dynamics in models \mathcal{M}_C and \mathcal{M}_S . More exactly, fixed points and their stability are discussed in Section 3, birth of low velocity n -cycles is investigated in Section 4 and birth of high velocity 3-cycles is studied in Section 5. In Section 6 the case of N impacts in one interval of the limiter's motion is studied for the model \mathcal{M}_C . We summarize our results in the last Section.

2 Bouncing ball: a simple motion of the table

Let a ball moves vertically in a constant gravitational field and collides with a periodically moving table. We treat the ball as a material point and assume that the limiter's mass is so large that its motion is not affected at impacts. Dynamics of the ball from an impact to the next impact can be described by the following Poincaré map in nondimensional form [25] (see also Ref. [11] where analogous map was derived earlier and Ref. [12] for generalizations of the bouncing ball model):

$$\gamma Y(T_{i+1}) = \gamma Y(T_i) - \Delta_{i+1}^2 + \Delta_{i+1} V_i, \quad (1a)$$

$$V_{i+1} = -RV_i + 2R\Delta_{i+1} + \gamma(1+R)\dot{Y}(T_{i+1}), \quad (1b)$$

where T_i denotes time of the i -th impact and V_i is the corresponding post-impact velocity while $\Delta_{i+1} \equiv T_{i+1} - T_i$. The parameters γ , R are a nondimensional acceleration and the coefficient of restitution, $0 \leq R < 1$ [5], respectively and the function $Y(T)$ represents the limiter's motion. The limiter's motion has been typically assumed in sinusoidal form, $Y_S(T) = \sin(2\pi T)$. Equations (1) and $Y = Y_S$ lead to the model \mathcal{M}_S . This choice of limiter's motion leads to serious difficulties in solving the first of Eqns.(1) for T_{i+1} , thus making analytical investigations of dynamics hardly possible. Accordingly, we have decided to simplify the limiter's periodic motion to make (1a) solvable. The function

$Y_C(T)$:

$$Y_C(T) = \begin{cases} f_1(T), & 0 \leq \hat{T} < \frac{1}{4} \\ f_2(T), & \frac{1}{4} \leq \hat{T} < \frac{1}{2} \\ f_3(T), & \frac{1}{2} \leq \hat{T} < \frac{3}{4} \\ f_4(T), & \frac{3}{4} \leq \hat{T} \leq 1 \end{cases} \quad (2)$$

$$f_1(T) = (32\pi - 128)\hat{T}^3 + (-16\pi + 48)\hat{T}^2 + 2\pi\hat{T} \quad (3a)$$

$$f_2(T) = (128 - 32\pi)\hat{T}^3 + (-144 + 32\pi)\hat{T}^2 + (48 - 10\pi)\hat{T} - 4 + \pi \quad (3b)$$

$$f_3(T) = (128 - 32\pi)\hat{T}^3 + (-240 + 64\pi)\hat{T}^2 + (144 - 42\pi)\hat{T} - 28 + 9\pi \quad (3c)$$

$$f_4(T) = (32\pi - 128)\hat{T}^3 + (336 - 80\pi)\hat{T}^2 + (-288 + 66\pi)\hat{T} + 80 - 18\pi \quad (3d)$$

approximates $Y_S = \sin(2\pi T)$ on the intervals $[k, k + 1]$, $k = 0, 1, \dots$, with $\hat{T} = T - [T]$, where $[x]$ is the floor function – the largest integer less than or equal to x . The model \mathcal{M}_C consists of equations (1), (2), (3) with control parameters R, γ . We shall also need velocities of the limiter, defined as $g_i(T) \stackrel{df}{=} \frac{d}{dt} f_i(T)$, $i = 1, \dots, 4$.

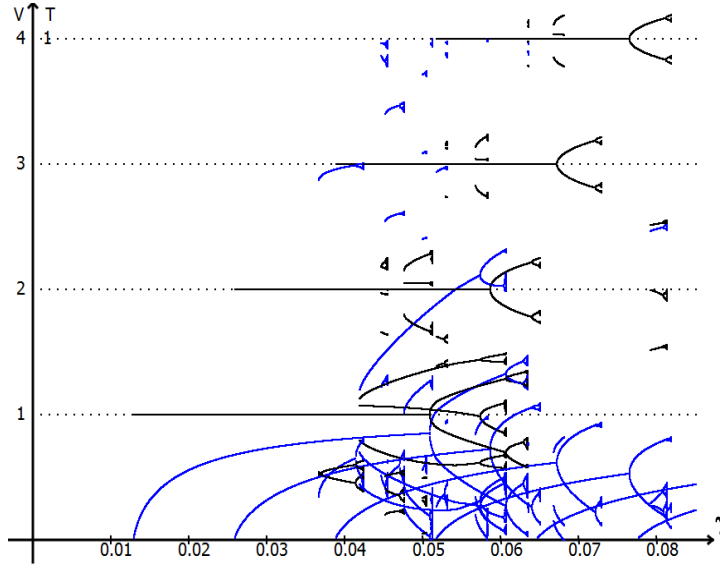


Figure 1: Bifurcation diagram for the model \mathcal{M}_C , $R = 0.85$.

In Fig. 1 above we show the bifurcation diagram with impact times (blue) and velocities (black) versus γ computed for growing γ and $R = 0.85$. It follows that dynamical system \mathcal{M}_C has several attractors: two fixed points which after one period doubling give rise to chaotic bands and two other fixed points which go to chaos via period doubling scenario. There are also several small attractors.

We shall investigate some of these attractors in the next Section combining analytical and numerical approach (general analytical conditions for birth of new modes of motion were given in [26]).

We show below the corresponding bifurcation diagram for the sinusoidal motion.

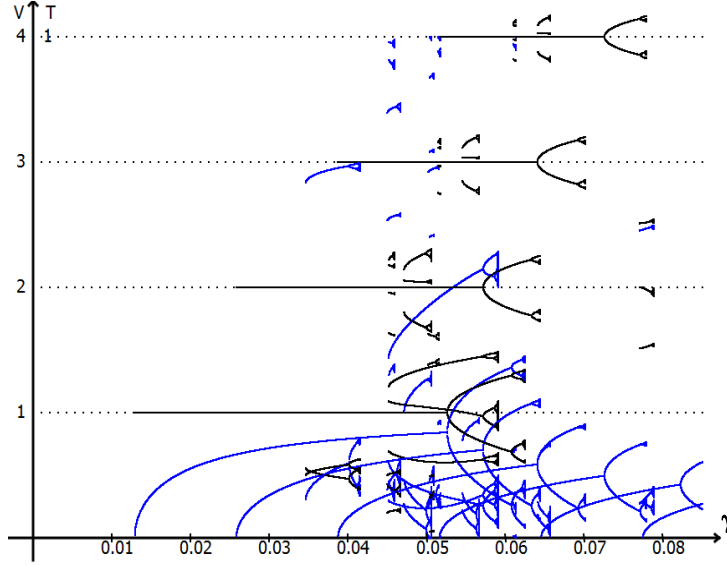


Figure 2: Bifurcation diagram for the model \mathcal{M}_S , $R = 0.85$.

Similarity of Figs. 1, 2 suggests that analytical results obtained for model \mathcal{M}_C shed light on the problem of sinusoidal motion, \mathcal{M}_S .

3 Fixed points and their stability

We shall first study periodic solutions of the model \mathcal{M}_C with one impact per k periods and $T \in (0, \frac{1}{4})$ since it is suggested by the bifurcation diagram that they are stable. Such states have to fulfill the following conditions:

$$V_{n+1} = V_n \equiv V_*^{(k/1)}, \quad T_{n+1} = T_n + k \equiv T_*^{(k/1)} + k \quad (k = 1, 2, \dots), \quad (4)$$

where:

$$T_*^{(k/1)} \in (0, \frac{1}{4}), \quad V_*^{(k/1)} > \gamma \dot{Y}_{c1} (T_*^{(k/1)}). \quad (5)$$

The demanded (stable) solution is given by

$$T_{*(s)}^{(k/1)} = \frac{\pi-3}{6(\pi-4)} - \frac{1}{24(\pi-4)} \sqrt{4(\pi-6)^2 + 6B(\pi-4)}, \quad \left(B = \frac{k}{\gamma} \frac{1-R}{1+R} \right) \quad (6a)$$

$$V_*^{(k/1)} = k. \quad (6b)$$

Since $T_* \in [0, 1]$ we demand that $T_* > 0$ and it follows from (6a) that physical solution appears for lower critical value $\gamma > \gamma_{cr1}^{(k/1)}$ where:

$$\gamma_{cr1,C}^{(k/1)} = \frac{k}{2\pi} \frac{1-R}{1+R}. \quad (7)$$

We have checked by stability analysis that the solution (6a), (6b) is stable for $\gamma > \gamma_{cr1,C}^{(k/1)}$, i.e. when it is physically acceptable. To determine upper critical value of γ when dynamics loses stability we put into (1):

$$T_i = T_{*(s)}^{(k/1)} + \varepsilon_i, \quad T_{i+1} = T_{*(s)}^{(k/1)} + k + \varepsilon_{i+1}, \quad (8)$$

$$V_i = V_* + \mu_i = k + \mu_i, \quad V_{i+1} = V_* + \mu_{i+1} = k + \mu_{i+1}, \quad (9)$$

with $Y(T)$ given by (3), and keep only terms linear in perturbations $\varepsilon_i, \varepsilon_{i+1}, \mu_i, \mu_{i+1}$ of the fixed point to get:

$$\begin{pmatrix} \varepsilon_{i+1} \\ \mu_{i+1} \end{pmatrix} = \begin{pmatrix} 1 & \frac{k}{\gamma f_1(T_*) + k} \\ \gamma(1+R)g_1(T_*) & k \frac{2R + \gamma(1+R)g_1(T_*)}{\gamma f_1(T_*) + k} - R \end{pmatrix} \begin{pmatrix} \varepsilon_i \\ \mu_i \end{pmatrix} \quad (10)$$

where $T_* \equiv T_{*(s)}^{(k/1)}$, $f_1(T)$ is given by (3a) and $g_1(T) = \frac{d}{dT} f_1(T)$.

Since the characteristic polynomial is:

$$\begin{aligned} X^2 + \alpha X + \beta &= 0 \\ \alpha &= 4\sqrt{4(\pi-6)^2 + 6k(\pi-4)\frac{1-R}{\gamma(1+R)}}(1+R)^2\gamma - R^2 - 1 \\ \beta &= R^2 \end{aligned} \quad (11)$$

application of the Shur-Cohn criterion ([27]):

$$\begin{aligned} \beta &< 1 \\ |\alpha| &< \beta + 1 \end{aligned} \quad (12)$$

leads finally to the localization of the fixed points (6), $\gamma_{cr1,C}^{(k/1)} < \gamma < \gamma_{cr2,C}^{(k/1)}$, with:

$$\gamma_{cr2,C}^{(k/1)} = \frac{6k(\pi-4)(R^2-1) + \sqrt{36k^2(\pi-4)^2(1-R^2)^2 + 4(\pi-6)^2(1+R^2)^2}}{8(\pi-6)^2(1+R)^2}, \quad R < 1. \quad (13)$$

In Fig. 3 stability regions in (R, γ) plane for the \mathcal{M}_C model are shown. In the case of the model \mathcal{M}_S we have:

$$\gamma_{cr2,S}^{(k/1)} = \gamma_{cr2,C}^{(k/1)}, \quad (14)$$

$$\gamma_{cr2,S}^{(k/1)} = \frac{\sqrt{k^2\pi^2(1-R^2)^2 + 4(1+R^2)^2}}{2\pi^2(1+R)^2}, \quad R < 1, \quad (15)$$

see [25] (note that in [25] we used $Y(T) = \sin(T)$ rather than $Y_S(T) = \sin(2\pi T)$ and it follows that all values of the control parameter λ must be rescaled, $\gamma = \frac{\lambda}{(2\pi)^2}$) and stability regions are very similar to those of model \mathcal{M}_C , cf. Fig. 4.

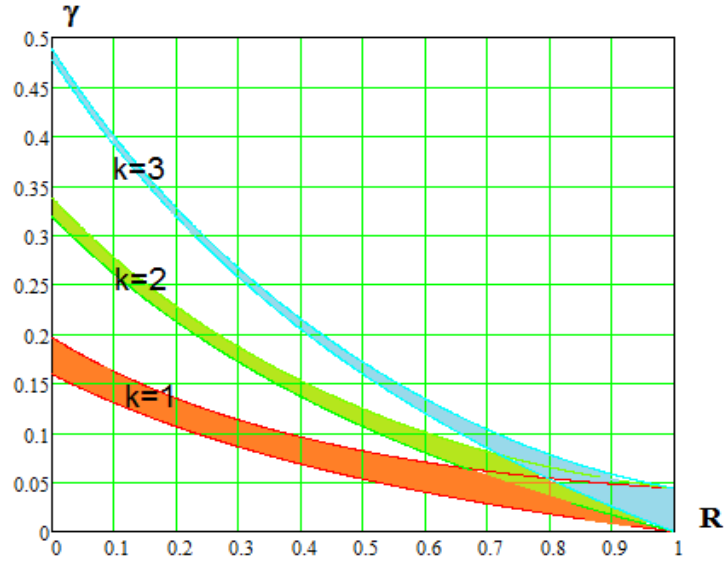


Figure 3: Stability regions in the (R, γ) plane, model \mathcal{M}_C .

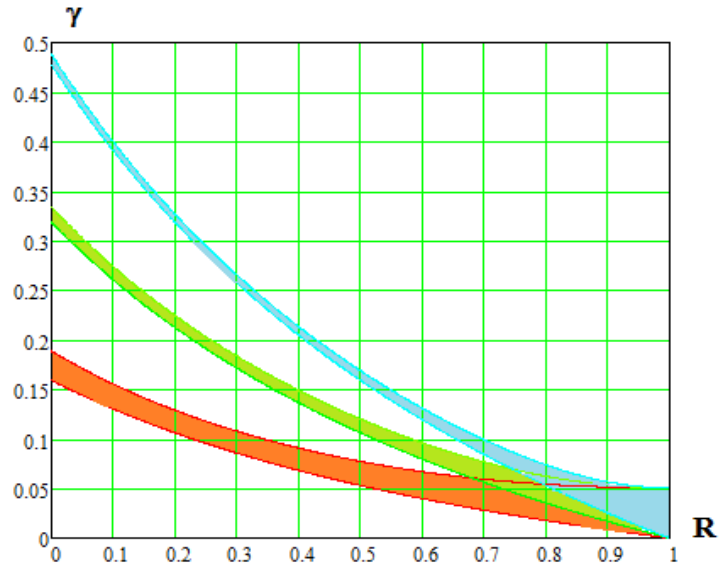


Figure 4: Stability regions in the (R, γ) plane, model \mathcal{M}_S .

4 Birth of low velocity k - cycles

In this Subsection we shall study birth of low velocity k - cycles which can be seen in the bifurcation diagrams, Figs. 1, 2, for $\gamma > 0.03$ and $V < 1$. In the case of such cycles $T_1, T_2, \dots, T_k \in (0, 1)$ and $T_{k+1} - 1 = T_1$. Of course, it is possible to follow periodic orbits backwards, i.e. iterating the map (1) until the convergence to the k - cycle is achieved for some initial condition and some γ . Then the value of γ is decreased (slightly) and the map is iterated again (until convergence is obtained) with the previously computed k - cycle as the initial condition. This method, although leads to determination of the critical value of γ at which the k - cycle disappears for decreasing γ (or is born for growing γ) but is time-consuming and not very effective due to very poor convergence near the threshold.

On the other hand, analytical conditions for birth of k - cycles are found below. In what follows theorems about differentiation of implicit functions [28] will turn out useful since Eqn. (1a) defines T_{i+1} implicitly. Consider equation:

$$F(T_1, T_2) = 0, \quad (16)$$

which defines dependence of, say, T_2 on T_1 , see [28] where necessary and sufficient assumptions are given. Then it follows from implicit function theorem that:

$$\frac{dT_2}{dT_1} = -\frac{F'_1}{F'_2}. \quad (17)$$

where $F'_1 \equiv \frac{\partial F}{\partial T_1}$, $F'_2 \equiv \frac{\partial F}{\partial T_2}$.

In a more complicated case, equations:

$$F(T_1, T_2, T_3) = 0, \quad G(T_1, T_2, T_3) = 0, \quad (18)$$

define T_2 and T_3 as functions of T_1 under appropriate assumptions. We can now compute derivatives with respect to T_1 as [28]:

$$\frac{\partial T_2}{\partial T_1} = -\frac{\det \begin{pmatrix} F'_1 & G'_1 \\ F'_3 & G'_3 \end{pmatrix}}{\det \begin{pmatrix} F'_2 & G'_2 \\ F'_3 & G'_3 \end{pmatrix}}, \quad \frac{\partial T_3}{\partial T_1} = -\frac{\det \begin{pmatrix} F'_2 & G'_2 \\ F'_1 & G'_1 \end{pmatrix}}{\det \begin{pmatrix} F'_2 & G'_2 \\ F'_3 & G'_3 \end{pmatrix}}, \quad (19)$$

with $F'_1 \equiv \frac{\partial F}{\partial T_1}$, $F'_2 \equiv \frac{\partial F}{\partial T_2}$, $F'_3 \equiv \frac{\partial F}{\partial T_3}$ and analogous notation for G'_i , $i = 1, 2, 3$.

4.1 Low velocity 2 - cycle in the model \mathcal{M}_C

Numerical tests show that a 2 - cycle fulfilling conditions $T_1 \in (0, \frac{1}{4})$, $T_2 \in (\frac{1}{2}, \frac{3}{4})$ and $T_3 = T_1 + 1$ is stable. This 2 - cycle can be seen in the bifurcation diagram in Fig. 1 for $\gamma \gtrsim 0.0366$ and $V_1 \cong 0.51$, $V_2 \cong 0.55$ ($R = 0.85$).

Equations to determine T_1 , T_2 and V_1 , V_2 are shown below:

$$\begin{aligned}
\gamma f_3(T_2) &= \gamma f_1(T_1) - (T_2 - T_1)^2 + (T_2 - T_1) V_1 \\
V_2 &= -RV_1 + 2R(T_2 - T_1) + \gamma(1 + R)g_3(T_2) \\
\gamma f_1(T_3 - 1) &= \gamma f_3(T_2) - (T_3 - T_2)^2 + (T_3 - T_2) V_2 \\
V_3 &= -RV_2 + 2R(T_3 - T_2) + \gamma(1 + R)g_1(T_3 - 1) \\
T_3 &= T_1 + 1 \\
V_3 &= V_1
\end{aligned} \tag{20}$$

where $f_i(T)$'s and $g_i(T)$'s are defined in Eqn. (3) and the text below.

We were able to simplify Eqns. (20) significantly obtaining equation for $\Delta \equiv T_2 - T_1$ only:

$$F(\Delta) = \sum_{j=0}^9 d_j \Delta^j = 0, \tag{21}$$

where d_i 's are given in the Appendix. Numerical computations suggest that the 2 - cycle appears for $\gamma = \gamma_{cr,C}^{(2)}$ and fixed R , where $\gamma_{cr,C}^{(2)}$ is a critical value, as a double (and stable) solution of Eqns. (20). For $\gamma > \gamma_{cr,C}^{(2)}$ there are two real solutions, one stable (seen in the bifurcation diagram) and another unstable. On the other hand, for $\gamma < \gamma_{cr,C}^{(2)}$ the solutions are complex conjugated and thus unphysical. Moreover, at $\gamma = \gamma_{cr,C}^{(2)}$ the stability matrix has unit eigenvalue. Therefore this is a tangent (saddle-node) bifurcation, see [29] for elementary discussion of the tangent bifurcation in the logistic map when the 3 - cycle is born. All other cycles discussed in our paper are also born in tangent bifurcation.

To determine critical value of the parameter γ let us note that double solution of the polynomial equation (21) is also the solution of $G(\Delta) = 0$ where $G(\Delta) = \frac{d}{d\Delta} F(\Delta)$. For example, solving for $R = 0.85$ the system of equations:

$$F(\Delta) = \sum_{j=0}^9 d_j \Delta^j = 0, \tag{22}$$

$$G(\Delta) = \sum_{j=1}^9 j d_j \Delta^{j-1} = 0, \tag{23}$$

we get $\gamma_{cr,C}^{(2)} = 0.03661705268289225062$, $\Delta_{cr} = 0.63427996067774735595$ (and many other, unphysical solutions) in perfect agreement with numerical computations, see also Fig. 1.

Alternatively, we can use implicit function theorem. Solving the second and fourth equations in (20) for V_1 , V_2 we get

$$\begin{aligned}
V_1 &= \frac{\gamma(1+R)(Rg_3(T_2) - g_1(T_1)) + 2R(1+R)(T_2 - T_1) - 2R}{-1 + R^2} \\
V_2 &= \frac{\gamma(1+R)(Rg_1(T_1) - g_3(T_2)) - 2R(1+R)(T_2 - T_1) + 2R^2}{-1 + R^2}
\end{aligned} \tag{24}$$

and

$$\begin{aligned}
F(T_1, T_2) &\stackrel{df}{=} \gamma f_1(T_1) - \gamma f_3(T_2) - (T_2 - T_1)^2 + (T_2 - T_1) V_1 = 0 \\
G(T_1, T_2) &\stackrel{df}{=} \gamma f_3(T_2) - \gamma f_1(T_1) - (T_1 + 1 - T_2)^2 + (T_1 + 1 - T_2) V_2 = 0
\end{aligned} \tag{25}$$

We can, in principle, solve the equation $F(T_1, T_2) = 0$ to determine $T_2(T_1)$ and demand that $\frac{d}{dT_1}G(T_1, T_2(T_1)) = 0$ to obtain condition for double root:

$$\begin{aligned} F(T_1, T_2) &= 0 \\ G(T_1, T_2) &= 0 \\ \frac{d}{dT_1}G(T_1, T_2) &= \frac{\partial}{\partial T_1}G(T_1, T_2) + \frac{\partial}{\partial T_1}G(T_1, T_2) \frac{dT_2}{dT_1} = 0 \end{aligned} \quad (26)$$

where the derivative $\frac{dT_2}{dT_1}$ is computed from Eqn. (17). Eqns. (26) provide analytical condition for the onset of the 2 - cycle. They are too complicated to be solved analytically but can be solved numerically for a fixed value of R or γ . For example, for $R = 0.85$ we compute the critical value of γ and the critical 2 - cycle: $T_1 = 8.1677488823442941327 \times 10^{-2}$, $T_2 = 0.71595744950119029728$, $\gamma_{cr,C}^{(2)} = 3.6617052682892250620 \times 10^{-2}$ in perfect agreement with solution of Eqns. (22), (23).

4.2 Low velocity 2 - cycle, model \mathcal{M}_S

We can apply this result to the case of sinusoidal motion. First of all, there is analogous 2 - cycle with $T_1 \in (0, \frac{1}{4})$, $T_2 \in (\frac{1}{2}, \frac{3}{4})$, which appears at $\gamma_{cr,S}^{(2)} \cong 0.0346$, see Fig. 2. It can be thus assumed that this 2 - cycle is also born as a double solution. The corresponding equations of the 2 - cycle are of form:

$$\begin{aligned} \gamma \sin(2\pi T_2) &= \gamma \sin(2\pi T_1) - (T_2 - T_1)^2 + (T_2 - T_1) V_1 \\ V_2 &= -RV_1 + 2R(T_2 - T_1) + \gamma(1 + R)2\pi \cos(2\pi T_2) \\ \gamma \sin(2\pi T_1) &= \gamma \sin(2\pi T_2) - (T_1 + 1 - T_2)^2 + (T_1 + 1 - T_2) V_2 \\ V_1 &= -RV_2 + 2R(T_1 + 1 - T_2) + \gamma(1 + R)2\pi \cos(2\pi T_1) \end{aligned} \quad (27)$$

Solving second and fourth equations of (27) for V_1, V_2 we get:

$$\begin{aligned} V_1 &= \frac{2}{1-R} \left(RT_1 - RT_2 + \gamma\pi \cos(2\pi T_1) - \gamma R\pi \cos(2\pi T_2) + \frac{R}{1+R} \right) \\ V_2 &= \frac{2}{1-R} \left(-RT_1 + RT_2 - \gamma R\pi \cos(2\pi T_1) + \gamma\pi \cos(2\pi T_2) - \frac{R^2}{1+R} \right) \end{aligned} \quad (28)$$

The problem is thus reduced to the system of two equations for T_1, T_2

$$\begin{aligned} F(T_1, T_2) &\stackrel{df}{=} \gamma \sin(2\pi T_1) - \gamma \sin(2\pi T_2) - \Delta^2 + V_1 \Delta = 0 \\ G(T_1, T_2) &\stackrel{df}{=} \gamma \sin(2\pi T_2) - \gamma \sin(2\pi T_1) - \tilde{\Delta}^2 + V_2 \tilde{\Delta} = 0 \\ \Delta &= T_2 - T_1, \quad \tilde{\Delta} = T_1 + 1 - T_2 \end{aligned} \quad (29)$$

We couldn't solve the system of equations (28), (29) analytically. Analytical condition for double root of these equations, i.e. for the beginning of the 2 - cycle, are again provided by Eqns. (26), (17) with functions F, G defined in (29). Solving now these equations numerically for $R = 0.85$ we get the critical value of the parameter γ and values of dynamical variables of the critical 2 - cycle: $\gamma_{cr,S}^{(2)} = 3.4580726363374620176 \times 10^{-2}$, $T_1 = 7.1712368607176410043 \times 10^{-2}$, $T_2 = 0.70698176135846385603$.

Numerical computations show that at $\gamma = \gamma_{cr,S}^{(2)}$ there is indeed a double solution of (27), two real solutions for $\gamma > \gamma_{cr,S}^{(2)}$ (one stable, another unstable) and complex solutions for $\gamma < \tilde{\gamma}_{cr}^{(2)}$. These considerations describe and explain the birth of the corresponding 2 - cycles.

4.3 Low velocity 3 - cycle in the model \mathcal{M}_C

We have found numerically that a 3 - cycle satisfying conditions $T_1 \in (0, \frac{1}{4})$, $T_2 \in (\frac{1}{2}, \frac{3}{4})$, $T_3 \in (\frac{3}{4}, 1)$ and $T_4 = T_1 + 1$ is stable. This attractor is seen in the bifurcation diagram near the 2 - cycle for $\gamma \gtrsim 0.0452$, $R = 0.85$, cf. Fig. 1. The 3 - cycle variables fulfill equations:

$$\begin{aligned}
\gamma f_3(T_2) &= \gamma f_1(T_1) - (T_2 - T_1)^2 + (T_2 - T_1) V_1 \\
V_2 &= -RV_1 + 2R(T_2 - T_1) + \gamma(1 + R)g_3(T_2) \\
\gamma f_4(T_3) &= \gamma f_3(T_2) - (T_3 - T_2)^2 + (T_3 - T_2) V_2 \\
V_3 &= -RV_2 + 2R(T_3 - T_2) + \gamma(1 + R)g_4(T_3) \\
\gamma f_1(T_4 - 1) &= \gamma f_4(T_3) - (T_4 - T_3)^2 + (T_4 - T_3) V_3 \\
V_4 &= -RV_3 + 2R(T_4 - T_3) + \gamma(1 + R)g_1(T_4 - 1) \\
T_4 &= T_1 + 1 \\
V_4 &= V_1
\end{aligned} \tag{30}$$

Equations (30) can be simplified. We can solve the second, fourth and sixth equations for V_1, V_2, V_3 to get

$$\begin{aligned}
V_1 &= \Gamma g_1(T_1) + \Gamma R^2 g_3(T_2) - \Gamma R g_4(T_3) + aT_1 + bT_2 - cT_3 + d \\
V_2 &= -\Gamma R g_1(T_1) + \Gamma g_3(T_2) + \Gamma R^2 g_4(T_3) - cT_1 + aT_2 + bT_3 - dR \\
V_3 &= \Gamma R^2 g_1(T_1) - \Gamma R g_3(T_2) + \Gamma g_4(T_3) + bT_1 - cT_2 + aT_3 + dR^2 \\
\Gamma &= \frac{\gamma}{R^2 - R + 1}, \quad a = \frac{2R(1-R)}{R^2 - R + 1}, \quad b = \frac{2R^2}{R^2 - R + 1}, \quad c = \frac{2R}{R^2 - R + 1}, \quad d = \frac{2R}{1 + R^3}
\end{aligned} \tag{31}$$

The problem is thus reduced to three equations for impact times T_1, T_2, T_3 only:

$$\begin{aligned}
F(T_1, T_2, T_3) &\stackrel{df}{=} \gamma f_1(T_1) - \gamma f_3(T_2) - \Delta_1^2 + \Delta_1 V_1 = 0 \\
G(T_1, T_2, T_3) &\stackrel{df}{=} \gamma f_3(T_2) - \gamma f_4(T_3) - \Delta_2^2 + \Delta_2 V_2 = 0 \\
H(T_1, T_2, T_3) &\stackrel{df}{=} \gamma f_4(T_3) - \gamma f_1(T_1) - \Delta_3^2 + \Delta_3 V_3 = 0 \\
&\Delta_1 = T_2 - T_1, \quad \Delta_2 = T_3 - T_2, \quad \Delta_3 = T_1 + 1 - T_3
\end{aligned} \tag{32}$$

where V_1, V_2, V_3 are known functions of impact times, cf. (31). We were unable to solve Eqns. (30) analytically. However, it is possible to write down condition for the onset of the 3 - cycle since it follows from numerical computations that the 3 - cycle is born as a double root of Eqns. (30). The condition for the double root is $\frac{d}{dT_1} H(T_1, T_2(T_1), T_3(T_1)) = 0$ and hence the condition for the

onset of the 3 – cycle is:

$$\begin{aligned}
F(T_1, T_2, T_3) &= 0 \\
G(T_1, T_2, T_3) &= 0 \\
H(T_1, T_2, T_3) &= 0 \\
\frac{d}{dT_1}H(T_1, T_2, T_3) &= \frac{\partial H}{\partial T_1} + \frac{\partial H}{\partial T_2} \frac{\partial T_2}{\partial T_1} + \frac{\partial H}{\partial T_3} \frac{\partial T_3}{\partial T_1} = 0
\end{aligned} \tag{33}$$

where the derivatives $\frac{\partial T_2}{\partial T_1}$, $\frac{\partial T_3}{\partial T_1}$ are computed from (19). Solving these equations numerically for $R = 0.85$ we get critical value of the control parameter γ and the critical 3 - cycle: $\gamma_{cr,C}^{(3)} = 4.5188344478468075539 \times 10^{-2}$, $T_1 = 0.10393159715396275497$, $T_2 = 0.63520026683019821215$, $T_3 = 0.84876032163157241499$.

4.4 Low velocity 3 - cycle in the model \mathcal{M}_S

We can apply this result to the case of sinusoidal motion. First of all, there is analogous 3 - cycle with $T_1 \in (0, \frac{1}{4})$, $T_2 \in (\frac{1}{2}, \frac{3}{4})$, $T_3 \in (\frac{3}{4}, 1)$ and $T_4 = T_1 + 1$, which appears at $\tilde{\gamma}_{cr}^{(3)} \cong 0.04499$, see Fig. 2. We can thus expect that this 3 - cycle is also born as a double solution. Dynamical variables of the 3 - cycle obey equations:

$$\begin{aligned}
\gamma \sin(2\pi T_2) &= \gamma \sin(2\pi T_1) - (T_2 - T_1)^2 + (T_2 - T_1) V_1 \\
V_2 &= -RV_1 + 2R(T_2 - T_1) + \gamma(1 + R)2\pi \cos(2\pi T_2) \\
\gamma \sin(2\pi T_3) &= \gamma \sin(2\pi T_2) - (T_3 - T_2)^2 + (T_3 - T_2) V_2 \\
V_3 &= -RV_2 + 2R(T_3 - T_2) + \gamma(1 + R)2\pi \cos(2\pi T_3) \\
\gamma \sin(2\pi T_1) &= \gamma \sin(2\pi T_3) - (T_1 + 1 - T_3)^2 + (T_1 + 1 - T_3) V_3 \\
V_1 &= -RV_3 + 2R(T_1 + 1 - T_3) + \gamma(1 + R)2\pi \cos(2\pi T_1)
\end{aligned} \tag{34}$$

Solving second, fourth and sixth equations for V_1, V_2, V_3 we get

$$\begin{aligned}
V_1 &= a(R^2 C_2 - RC_3 + C_1) + b(R(T_2 - T_1) + T_1 - T_3) + c \\
V_2 &= a(R^2 C_3 - RC_1 + C_2) + b(R(T_3 - T_2) + T_2 - T_1) - cR \\
V_3 &= a(R^2 C_1 - RC_2 + C_3) + b(R(T_1 - T_3) + T_3 - T_2) + cR^2 \\
a &= \frac{2\gamma\pi(1+R)}{1+R^3}, \quad b = \frac{2R(1+R)}{1+R^3}, \quad c = \frac{2R}{1+R^3}, \quad C_i = \cos 2\pi T_i \quad (i = 1, 2, 3)
\end{aligned} \tag{35}$$

and we have to solve equations for impact times only:

$$\begin{aligned}
F(T_1, T_2, T_3) &\stackrel{df}{=} \gamma \sin(2\pi T_1) - \gamma \sin(2\pi T_2) - \Delta_1^2 + \Delta_1 V_1 = 0 \\
G(T_1, T_2, T_3) &\stackrel{df}{=} \gamma \sin(2\pi T_2) - \gamma \sin(2\pi T_3) - \Delta_2^2 + \Delta_2 V_2 = 0 \\
H(T_1, T_2, T_3) &\stackrel{df}{=} \gamma \sin(2\pi T_3) - \gamma \sin(2\pi T_1) - \Delta_3^2 + \Delta_3 V_3 = 0 \\
\Delta_1 &= T_2 - T_1, \quad \Delta_2 = T_3 - T_2, \quad \Delta_3 = T_1 + 1 - T_3
\end{aligned} \tag{36}$$

Equations (35), (36) are too complicated to be solved analytically. However, it is possible to write down condition for the beginning of the 3 - cycle since it follows from numerical computations that the 3 - cycle is born as a double root

of Eqns. (34). More exactly, we have to solve Eqns. (33) for functions F, G, H defined in (36). We thus get for $R = 0.85$ the critical value $\gamma_{cr,S}^{(3)} = 4.498\,669\,496\,445\,746\,754\,8 \times 10^{-2}$ and the critical 3 - cycle, $T_1 = 9.514\,258\,132\,574\,445\,543\,3 \times 10^{-2}$, $T_2 = 0.633\,092\,075\,481\,873\,314\,56$, $T_3 = 0.848\,082\,849\,264\,211\,982\,09$.

5 Birth of high velocity 3 - cycles

High velocity 3 - cycles are very characteristic of bouncing ball dynamics. They accompany all fixed points and are seen in the bifurcation diagrams around $V = 1, 2, 3, \dots$, see Figs. 1, 2. In the case of such cycles $T_1, T_2, T_3 \in (0, 1)$ and $T_4 - k = T_1$.

5.1 Model \mathcal{M}_C , $V \cong 1$

We start with such 3 - cycle with $V \cong 1$ which appears in the model \mathcal{M}_C for $\gamma \gtrsim 0.042$, see Fig. 1 with impact times $T_1 \in (\frac{1}{4}, \frac{1}{2})$, $T_2 - 1 \in (0, \frac{1}{4})$, $T_3 - 1 \in (0, \frac{1}{4})$, $T_4 - 1 = T_1$. The corresponding equations are:

$$\begin{aligned} \gamma f_1(T_2 - 1) &= \gamma f_2(T_1) - (T_2 - T_1)^2 + (T_2 - T_1) V_1 \\ V_2 &= -RV_1 + 2R(T_2 - T_1) + \gamma(1 + R)g_1(T_2 - 1) \\ \gamma f_1(T_3 - 1) &= \gamma f_1(T_2 - 1) - (T_3 - T_2 + 1)^2 + (T_3 - T_2 + 1) V_2 \\ V_3 &= -RV_2 + 2R(T_3 - T_2 + 1) + \gamma(1 + R)g_1(T_3 - 1) \\ \gamma f_2(T_1) &= \gamma f_1(T_3 - 1) - (T_1 + 2 - T_3)^2 + (T_1 + 2 - T_3) V_3 \\ V_1 &= -RV_3 + 2R(T_1 + 1 - T_3 + 1) + \gamma(1 + R)g_2(T_1) \end{aligned} \quad (37)$$

Solving equations for V_1, V_2, V_3 we get

$$\begin{aligned} V_1 &= a\gamma g_2(T_1) - aR\gamma g_1(T_3 - 1) + aR^2\gamma g_1(T_2 - 1) - 2aRA_1 + b \\ V_2 &= \gamma a g_1(T_2 - 1) - aR\gamma g_2(T_1) + a\gamma R^2 g_1(T_3 - 1) - 2aRA_2 - b \\ V_3 &= a\gamma g_1(T_3 - 1) - aR\gamma g_1(T_2 - 1) + a\gamma R^2 g_2(T_1) + 2aRA_3 + c \\ A_1 &= -RT_2 + RT_1 - T_1 + T_3, \quad A_2 = -RT_3 + RT_2 - T_2 + T_1 \\ A_3 &= -RT_3 + RT_1 - T_2 + T_3 \\ a &= \frac{(1+R)}{1+R^3}, \quad b = \frac{2R(2-R)}{1+R^3}, \quad c = \frac{2R(1+2R^2)}{1+R^3} \end{aligned} \quad (38)$$

and

$$\begin{aligned} F_1(T_1, T_2, T_3) &\stackrel{df}{=} \gamma f_2(T_1) - \gamma f_1(T_2 - 1) - \Delta_1^2 + \Delta_1 V_1 = 0 \\ F_2(T_1, T_2, T_3) &\stackrel{df}{=} \gamma f_1(T_2 - 1) - \gamma f_1(T_3 - 1) - \Delta_2^2 + \Delta_2 V_2 = 0 \\ F_3(T_1, T_2, T_3) &\stackrel{df}{=} \gamma f_1(T_3 - 1) - \gamma f_2(T_1) - \Delta_3^2 + \Delta_3 V_3 = 0 \\ \Delta_1 &= T_2 - T_1, \quad \Delta_2 = T_3 - T_2 + 1, \quad \Delta_3 = T_1 + 2 - T_3 \end{aligned} \quad (39)$$

Analytical condition for the onset of this 3 - cycle is given by Eqns. (33) with F, G, H given by (39). Solving these equations numerically for $R = 0.85$ we get $\gamma_{cr}^{(3,1)} = 4.184\,258\,672\,013\,445\,046\,3 \times 10^{-2}$ and $T_1 = 0.292\,944\,344\,346\,867\,579\,94$, $T_2 = 1.113\,429\,439\,708\,681\,876\,6$, $T_3 = 1.179\,198\,676\,090\,233\,556\,9$. For $R_{cr,C} =$

0.685 101 194 and $\gamma_{cr,C} = 0.056 81 9 493$ there is smooth transition to the state $T_1 \in (\frac{1}{4}, \frac{1}{2})$, $T_2 \in (\frac{3}{4}, 1)$, $T_3 - 1 \in (0, \frac{1}{4})$, $T_4 - 1 = T_1$. For $R > R_{cr,C}$ this transition occurs for $\gamma > \gamma_{cr,C}$.

5.2 Model \mathcal{M}_S , $V \cong 1$

In the case of sinusoidal motion described by the model \mathcal{M}_C we can see the 3 – cycle with $V \cong 1$ in Fig. 2 for $\gamma \gtrsim 0.045$ with impact times $T_1 \in (0, \frac{1}{4})$, $T_2 - 1 \in (\frac{1}{4}, \frac{1}{2})$, $T_3 - 1 \in (0, \frac{1}{4})$, $T_4 - 1 = T_1$. Dynamical equations read:

$$\begin{aligned} \gamma \sin(2\pi T_2) &= \gamma \sin(2\pi T_1) - (T_2 - T_1)^2 + (T_2 - T_1) V_1 \\ V_2 &= -RV_1 + 2R(T_2 - T_1) + \gamma(1 + R)2\pi \cos(2\pi T_2) \\ \gamma \sin(2\pi T_3) &= \gamma \sin(2\pi T_2) - (T_3 - T_2 + 1)^2 + (T_3 - T_2 + 1) V_2 \\ V_3 &= -RV_2 + 2R(T_3 - T_2 + 1) + \gamma(1 + R)2\pi \cos(2\pi T_3) \\ \gamma \sin(2\pi T_1) &= \gamma \sin(2\pi T_3) - (T_1 + 2 - T_3)^2 + (T_1 + 2 - T_3) V_3 \\ V_1 &= -RV_3 + 2R(T_1 + 2 - T_3) + \gamma(1 + R)2\pi \cos(2\pi T_1) \end{aligned} \quad (40)$$

Solving equations for V_1 , V_2 , V_3 we get

$$\begin{aligned} V_1 &= aR^2 \cos 2\pi T_2 - aR \cos 2\pi T_3 + a \cos 2\pi T_1 - bA_1 - c \\ V_2 &= aR^2 \cos 2\pi T_3 - aR \cos 2\pi T_1 + a \cos 2\pi T_2 - bA_2 + cR \\ V_3 &= aR^2 \cos 2\pi T_1 - aR \cos 2\pi T_2 + a \cos 2\pi T_3 + bA_3 + d \\ A_1 &= -RT_2 + RT_1 - T_1 + T_3, \quad A_2 = -RT_3 + RT_2 - T_2 + T_1 \\ A_3 &= RT_1 - RT_3 + T_3 - T_2 \\ a &= \frac{2\gamma\pi(1+R)}{1+R^3}, \quad b = \frac{2R(1+R)}{1+R^3}, \quad c = \frac{2R(R-2)}{1+R^3}, \quad d = \frac{2R(1+2R^2)}{1+R^3} \end{aligned} \quad (41)$$

and

$$\begin{aligned} F(T_1, T_2, T_3) &\stackrel{df}{=} \gamma \sin(2\pi T_1) - \gamma \sin(2\pi T_2) - \Delta_1^2 + \Delta_1 V_1 = 0 \\ G(T_1, T_2, T_3) &\stackrel{df}{=} \gamma \sin(2\pi T_2) - \gamma \sin(2\pi T_3) - \Delta_2^2 + \Delta_2 V_2 = 0 \\ H(T_1, T_2, T_3) &\stackrel{df}{=} \gamma \sin(2\pi T_3) - \gamma \sin(2\pi T_1) - \Delta_3^2 + \Delta_3 V_3 = 0 \\ \Delta_1 &= T_2 - T_1, \quad \Delta_2 = T_3 - T_2 + 1, \quad \Delta_3 = T_1 - T_3 + 2 \end{aligned} \quad (42)$$

Conditions for the onset of 3 – cycle are given by Eqns. (33) with functions F , G , H defined in (42). Solving these equations for $R = 0.85$ we obtain: $\tilde{\gamma}_{cr}^{(3,1)} = 4.514 020 805 615 479 834 1 \times 10^{-2}$ and $T_1 = 7.439 906 099 929 247 941 1 \times 10^{-2}$, $T_2 = 1.154 226 438 813 261 052 6$, $T_3 = 1.357 478 350 324 075 728 9$. For $R_{cr,S} = 0.691 964 922 5$ and $\gamma_{cr,S} = 0.055 974 756$ there is smooth transition to the state $T_1 \in (\frac{1}{4}, \frac{1}{2})$, $T_2 \in (\frac{3}{4}, 1)$, $T_3 - 1 \in (0, \frac{1}{4})$, $T_4 - 1 = T_1$. For $R > R_{cr,S}$ this transition occurs for $\gamma > \gamma_{cr,S}$.

6 N impacts in one period of limiter's motion and chattering in the model \mathcal{M}_C

In the bouncing ball dynamics chattering and chaotic dynamics arise typically, see [30, 31] where chattering mechanism was studied numerically for sinusoidal

motion of the table. Due to simplicity of our model analytical computations are possible.

We shall consider a possible course of events after grazing.

6.1 First interval: $T_i, T_{i+1} \in (0, \frac{1}{4})$

Let $T_i, T_{i+1} \in (0, \frac{1}{4})$. In this case we get from Eqns. (1a), (3a) $\Delta_{i+1} = 0$ and:

$$\Delta_{i+1}^{(\pm)} = \frac{\frac{1}{2}\gamma a_1(T_i) + 1}{64\gamma(4-\pi)} \left(1 \pm \sqrt{1 - \frac{128\gamma(4-\pi)W_i}{(\frac{1}{2}\gamma a_1(T_i) + 1)^2}} \right), \quad (43)$$

$$a_1(T) = \frac{d^2}{dT^2} f_1(T),$$

and $\Delta_{i+1}^{(-)}$ is the solution describing chattering (obviously, W_i must be small enough so that expression under the square root be non-negative). The denominator in (43) can be written as $\frac{1}{2}\gamma a_1(T_i) + 1 = -96\gamma(4-\pi)(T_i - T_{cr}^{(1)})$ where:

$$T_{cr}^{(1)} = \frac{-1 + 16\gamma(-3 + \pi)}{96\gamma(-4 + \pi)}, \quad (44)$$

and we check that $T_{cr}^{(1)} \leq \frac{1}{4}$ occurs for $\gamma \geq \gamma_{cr}^{(1)} = 0.043731$. Therefore for $\gamma < \gamma_{cr}$ the grazing ball will stay on the table forever. Let us assume that a ball sticks to the table for some time $T_g < T_{cr}^{(1)} \leq \frac{1}{4}$. At critical point $T_i = T_{cr}^{(1)}$ and $V_i = \gamma g_1(T_i)$, equations (1a), (3a) have the degenerate triple solution $T_{i+1} = T_{cr}^{(1)}$. For $\gamma > \gamma_{cr}^{(1)}$ and $T > T_{cr}^{(1)}$ the solution $\Delta_{i+1}^{(-)}$ is no longer valid since $\frac{1}{2}\gamma a_1(T_i) + 1 < 0$ and $\Delta_{i+1}^{(-)} < 0$ what is physically unacceptable. The solution $\Delta_{i+1}^{(+)}$ is also unacceptable and thus the ball has to jump to another time interval, $(\frac{1}{4}, \frac{1}{2})$, $(\frac{1}{2}, \frac{3}{4})$ or further. We shall now consider the first possibility. Let us assume that the ball grazes at $T_i = T_{cr}^{(1)}$ and thus its velocity is that of the table, $V_i = \gamma g_1(T_i)$. We thus have to solve equation for the jump:

$$\begin{aligned} \gamma f_2(T_{i+1}) &= \gamma f_1(T_i) - (T_{i+1} - T_i)^2 + (T_{i+1} - T_i) V_i, \\ T_i &= T_{cr}^{(1)} \in (0, \frac{1}{4}), \quad T_{i+1} \in (\frac{1}{4}, \frac{1}{2}), \quad V_i = \gamma g_1(T_i). \end{aligned} \quad (45)$$

The solution of (45) is

$$T_{cr}^{(1 \rightarrow 2)} = \frac{(\frac{\pi}{12} - \frac{1}{2}) \left(4 + 2^{\frac{2}{3}} + \sqrt[3]{2} \right) + \frac{1}{2}}{-4 + \pi} \gamma + \frac{1 + 2^{\frac{2}{3}} + \sqrt[3]{2}}{96(-4 + \pi)\gamma}. \quad (46)$$

It follows that the interval $(T_{cr}^{(1)}, T_{cr}^{(1 \rightarrow 2)})$ is the forbidden zone. The solution (50) is valid for $\gamma \leq \gamma_{cr}^{(1 \rightarrow 2)} = 0.057102$ since for $\gamma > \gamma_{cr}^{(2)}$ we have $T_{cr}^{(1 \rightarrow 2)} > \frac{1}{2}$ contradicting assumptions. For $\gamma > \gamma_{cr}^{(1 \rightarrow 2)}$ we thus have to consider the following equation for the jump to time interval $(\frac{1}{2}, \frac{3}{4})$:

$$\begin{aligned} \gamma f_3(T_{i+1}) &= \gamma f_1(T_i) - (T_{i+1} - T_i)^2 + (T_{i+1} - T_i) V_i, \\ T_i &= T_{cr}^{(1)} \in (0, \frac{1}{4}), \quad T_{i+1} \in (\frac{1}{2}, \frac{3}{4}), \quad V_i = \gamma g_1(T_i). \end{aligned} \quad (47)$$

Solution of Eqn. (47), $X = T_{cr}^{(1 \rightarrow 3)}$, fulfills the following cubic equation:

$$\begin{aligned} a_0 X^3 + (b_0 + b_1 \gamma) X^2 + (c_0 + c_1 \gamma + c_2 \gamma^2) X + d_0 + d_1 \gamma + d_2 \gamma^2 + d_3 \gamma^3 &= 0 \\ a_0 = 32, \quad b_0 = 1, \quad b_1 = -240 + 64\pi, \quad c_0 = \frac{1}{96}, \quad c_1 = 1 - \frac{1}{3}\pi \\ c_2 = 304\pi - 552 - \frac{124}{3}\pi^2, \quad d_0 = \frac{1}{27 \cdot 648}, \quad d_1 = -\frac{1}{576}\pi + \frac{1}{192}, \\ d_2 = \frac{1}{36}\pi^2 - \frac{1}{6}\pi + \frac{1}{4}, \quad d_3 = \frac{239}{27}\pi^3 - \frac{296}{3}\pi^2 + 364\pi - 444 \end{aligned} \quad (48)$$

with $T_{cr}^{(1 \rightarrow 3)} = \frac{X}{\gamma(-4+\pi)}$. Eqn. (52) has acceptable solutions, i.e. such that $T_{cr}^{(1 \rightarrow 3)} \in (\frac{1}{2}, \frac{3}{4})$, for $\gamma \leq \gamma_{cr}^{(1 \rightarrow 3)} = 0.087308825$.

6.2 Second interval: $T_i, T_{i+1} \in (\frac{1}{4}, \frac{1}{2})$

We have to consider now chattering in the interval $(\frac{1}{4}, \frac{1}{2})$. Let us thus consider that $T_i, T_{i+1} \in (\frac{1}{4}, \frac{1}{2})$. It follows from equations (1a), (3b) that $\Delta_{i+1} = 0$ and

$$\begin{aligned} \Delta_{i+1}^{(\pm)} &= \frac{\frac{1}{2}\gamma a_2(T_i) + 1}{64\gamma(4-\pi)} \left(-1 \pm \frac{\frac{1}{2}\gamma a_2(T_i) + 1}{|\frac{1}{2}\gamma a_2(T_i) + 1|} \sqrt{1 + \frac{128\gamma(4-\pi)W_i}{(\frac{1}{2}\gamma a_2(T_i) + 1)^2}} \right), \\ a_2(T) &= \frac{d^2}{dT^2} f_2(T). \end{aligned} \quad (49)$$

The solution describing chattering is $\Delta_{i+1}^{(+)}$ for $\frac{1}{2}\gamma a_2(T_i) + 1 > 0$. The denominator can be written in form $\frac{1}{2}\gamma a_2(T_i) + 1 = 96\gamma(4-\pi)(T - T_{cr}^{(2)})$ where:

$$T_{cr}^{(2)} = \frac{1}{96} \frac{1 - 144\gamma + 32\gamma\pi}{\gamma(\pi - 4)}. \quad (50)$$

It follows that chattering is thus possible for $T_i \in (T_{cr}^{(2)}, \frac{1}{2})$.

6.3 Third interval: $T_i, T_{i+1} \in (\frac{1}{2}, \frac{3}{4})$

Let us suppose now that $T_i, T_{i+1} \in (\frac{1}{2}, \frac{3}{4})$. It follows from equations (1a), (3c) that $\Delta_{i+1} = 0$ and

$$\begin{aligned} \Delta_{i+1}^{(\pm)} &= \frac{\frac{1}{2}\gamma a_3(T_i) + 1}{64\gamma(4-\pi)} \left(-1 \pm \frac{\frac{1}{2}\gamma a_3(T_i) + 1}{|\frac{1}{2}\gamma a_3(T_i) + 1|} \sqrt{1 + \frac{128\gamma(4-\pi)W_i}{(\frac{1}{2}\gamma a_3(T_i) + 1)^2}} \right), \\ a_3(T) &= \frac{d^2}{dT^2} f_3(T). \end{aligned} \quad (51)$$

The solution describing chattering is $\Delta_{i+1}^{(+)}$ for $\frac{1}{2}\gamma a_3(T_i) + 1 > 0$. The denominator can be written in form $\frac{1}{2}\gamma a_3(T_i) + 1 = 96\gamma(4-\pi)(T - T_{cr}^{(3)})$ with:

$$T_{cr}^{(3)} = \frac{1}{96} \frac{-240\gamma + 64\gamma\pi + 1}{\gamma(\pi - 4)} < 0.5 \quad (\gamma > 0), \quad (52)$$

and it follows that $T_{cr}^{(3)}$ cannot belong to $(\frac{1}{2}, \frac{3}{4})$ interval for positive γ . Chattering is thus possible in the whole interval $(\frac{1}{2}, \frac{3}{4})$ since $\frac{1}{2}\gamma a_3(T_i) + 1 > 0$.

6.4 Fourth interval: $T_i, T_{i+1} \in (\frac{3}{4}, 1)$

Let us assume finally that two subsequent impacts occur in the last quarter-period and $T_i, T_{i+1} \in (\frac{3}{4}, 1)$. In this case the solution $\Delta_{i+1} = 0$ of equation (1a) is always present and this equation can be easily solved. We thus get from Eqns. (1a), (3d) $\Delta_{i+1} = 0$ and:

$$\Delta_{i+1}^{(\pm)} = \frac{\frac{1}{2}\gamma a_4(T_i) + 1}{64\gamma(4-\pi)} \left(1 \pm \sqrt{1 - \frac{128\gamma(4-\pi)W_i}{(\frac{1}{2}\gamma a_4(T_i) + 1)^2}} \right), \quad (53)$$

$$a_4(T_i) = \frac{d^2}{dT^2} f_4(T), \quad (54)$$

where $\gamma a_4(T_i)$ is the acceleration of the table, $a_4(T) = \frac{d^2}{dT^2} f_4(T)$ and W_i is a relative velocity, $W_i = V_i - \gamma \frac{d}{dT_i} f_4(T_i)$. In the case of chattering the appropriate solution is $\Delta_{i+1}^{(-)}$ since for $W_i \rightarrow 0$ we have $\Delta_{i+1}^{(-)} \rightarrow 0$. The denominator can be written as $\frac{1}{2}\gamma a_4(T_i) + 1 = -96\gamma(4-\pi) \left(T - T_{cr}^{(4)} \right)$ where

$$T_{cr}^{(4)} = \frac{1}{96} \frac{16\gamma(21-5\pi) + 1}{\gamma(4-\pi)} > 1 \quad (\gamma > 0). \quad (55)$$

We do not have to worry that the denominator in (53) may vanish since the condition $\frac{1}{2}\gamma a_4(T_i) + 1 = 0$ cannot be fulfilled for $T_i \in (\frac{3}{4}, 1)$ and $\gamma > 0$. Therefore chattering is possible in the whole interval $(\frac{1}{2}, \frac{3}{4})$ since $\frac{1}{2}\gamma a_4(T_i) + 1 > 0$.

6.5 Grazing: a homoclinic orbit

Let us assume that the ball grazes at $T_i = T_{cr}^{(1)}$ with velocity $V_i = \gamma g_1(T_i)$ (i.e. it has velocity of the table) and that the value of γ is such that the ball jumps. Let us next assume that the ball grazes at some time T_* in the interval $\left[0, T_{cr}^{(1)}\right]$.

For growing γ it will happen eventually at $\gamma = \gamma_*$ that $T_* = T_{cr}^{(1)}$. Then for larger values of γ the ball after grazing and jumping returns with chattering into the $(0, T_{cr}^{(1)})$ interval but it will not graze, i.e. V_* will be larger than $\gamma g_1(T_*)$. We have computed numerically the critical value as $\gamma_* = 0.0583486$. Therefore for $\gamma > \gamma_*$ long transients can be expected after grazing.

In Fig. 5 below bifurcation diagram is shown with initial conditions on the grazing manifold. For $\gamma < \gamma_*$ the grazing manifold is globally attractive. Indeed, in this parameter range the bifurcation diagram is empty (we show attractors different than the grazing manifold only). On the other hand, for $\gamma > \gamma_*$ the ball jumps at $T = T_{cr}^{(1)}$ and then either grazes eventually or settles on some attractor after a long transient. Just after the threshold there is a very irregular, probably chaotic attractor.

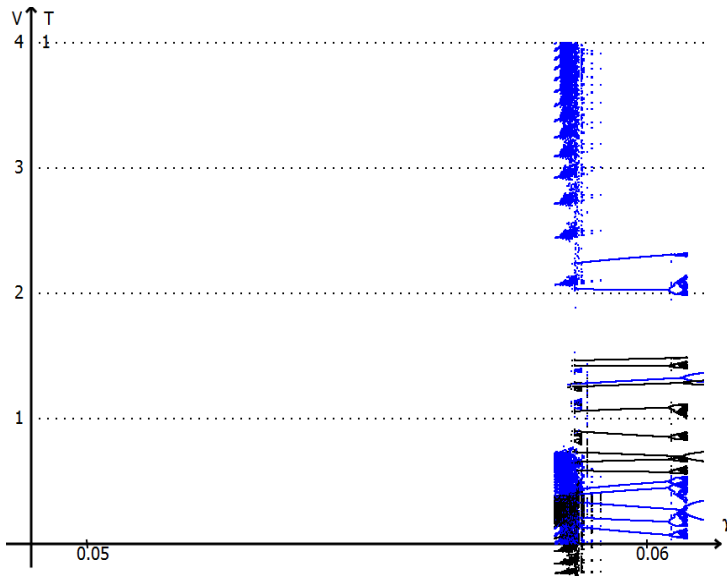


Figure 5: Bifurcation diagram for the model \mathcal{M}_C , $R = 0.85$. Initial conditions are on the grazing manifold.

7 Summary

We have studied dynamics of a bouncing ball impacting with a periodically moving limiter within two frameworks of the table motion: \mathcal{M}_C and \mathcal{M}_S defined in Section 2. Stability conditions of fixed points have been determined and results for the models \mathcal{M}_C and \mathcal{M}_S have been compared. Then we have found that low-velocity k -cycles as well as high-velocity 3-cycles are generically born in tangent bifurcations. Moreover, we have been able using implicit functions theorems, to write down conditions for the onset of these cycles and solve them numerically. Analytical conditions for the onset of such cycles are new.

Finally, the case of N impacts in one interval of the limiter's motion has been studied within the \mathcal{M}_C model. Equations for N impacts in one period of limiter's motion were found and simplified significantly, making analysis of chattering and grazing possible. We have found, combining analytical and numerical approach, the grazing homoclinic orbit which appears at $\gamma = \gamma_*$ and gives rise to a very irregular, probably chaotic attractor, cf. Fig. 5. We expect that analogous attractor exists in the model \mathcal{M}_S .

A Equation for the 2 - cycle

In the Appendix coefficients of the polynomial (21) are listed.

$$d_9 = 2^{16}3^3\gamma^3(-4 + \pi)^4(1 + R)^6$$

$$d_8 = -2^{12}3^3\gamma^2(1 + R)^6(-4 + \pi)^3((72\pi - 288)\gamma + 1)$$

$$d_7 = 2^63^3\gamma(1 + R)^4(-4 + \pi)^2(a_2R^2 + a_1R + a_0)$$

$$a_2 = (-66\,048\pi + 8256\pi^2 + 132\,096)\gamma^2 + (256\pi - 1024)\gamma + 1$$

$$a_1 = (-138\,240\pi + 17\,280\pi^2 + 276\,480)\gamma^2 + 2 + (512\pi - 2048)\gamma$$

$$a_0 = (-66\,048\pi + 8256\pi^2 + 132\,096)\gamma^2 + (256\pi - 1024)\gamma + 1$$

$$d_6 = -8(1 + R)^4(-4 + \pi)(b_2R^2 + b_1R + b_0)$$

$$b_2 = (-19\,160\,064\pi^2 + 76\,640\,256\pi + 1596\,672\pi^3 - 102\,187\,008)\gamma + (-3024 + 756\pi)\gamma + (1361\,664 - 679\,680\pi + 84\,864\pi^2)\gamma^2 + 1$$

$$b_1 = (-241\,532\,928 + 3773\,952\pi^3 + 181\,149\,696\pi - 45\,287\,424\pi^2)\gamma^3 + (183\,552\pi^2 - 1469\,952\pi + 2944\,512)\gamma^2 + (1512\pi - 6048)\gamma + 2$$

$$b_0 = (-19\,160\,064\pi^2 + 76\,640\,256\pi + 1596\,672\pi^3 - 102\,187\,008)\gamma^3 + (1361\,664 - 679\,680\pi + 84\,864\pi^2)\gamma^2 + (-3024 + 756\pi)\gamma + 1$$

$$d_5 = 8(1 + R)^4(c_2R^2 + c_1R + c_0)$$

$$c_2 = (180\,983\,808 - 180\,983\,808\pi - 11\,319\,552\pi^3 + 707\,968\pi^4 + 67\,885\,056\pi^2)\gamma^3 + (2951\,424\pi - 3953\,664 + 61\,056\pi^3 - 734\,976\pi^2)\gamma^2 + (17\,928 + 1118\pi^2 - 8952\pi)\gamma + 3\pi - 12$$

$$c_1 = (2202\,368\pi^4 + 565\,014\,528 - 564\,682\,752\pi + 211\,636\,224\pi^2 - 35\,254\,272\pi^3)\gamma^3 + (163\,584\pi^3 - 10\,561\,536 - 1967\,616\pi^2 + 7893\,504\pi)\gamma^2 + (-16\,176\pi + 32\,400 + 2020\pi^2)\gamma - 24 + 6\pi$$

$$c_0 = (706\,432\pi^4 + 68\,106\,240\pi^2 - 181\,979\,136\pi - 11\,327\,232\pi^3 + 182\,310\,912)\gamma^3 + (2951\,424\pi - 3953\,664 + 61\,056\pi^3 - 734\,976\pi^2)\gamma^2 + (17\,928 + 1118\pi^2 - 8952\pi)\gamma + 3\pi - 12$$

$$\begin{aligned}
d_4 &= -4(1+R)^2(e_4R^4 + e_3R^3 + e_2R^2 + e_1R + e_0) \\
e_4 &= (50\,264\,064 - 3181\,824\pi^3 + 201\,344\pi^4 - 50\,264\,064\pi + 18\,929\,664\pi^2)\gamma^3 + \\
&\quad (1854\,720\pi - 2515\,968 - 456\,960\pi^2 + 37\,632\pi^3)\gamma^2 + \\
&\quad (29\,160 - 14\,520\pi + 1810\pi^2)\gamma - 36 + 9\pi \\
e_3 &= (-29\,354\,496\pi^3 + 473\,112\,576 + 176\,357\,376\pi^2 + 1834\,496\pi^4 - 471\,453\,696\pi)\gamma^3 + \\
&\quad (-2864\,640\pi^2 + 11\,566\,080\pi - 15\,593\,472 + 236\,928\pi^3)\gamma^2 + \\
&\quad (6160\pi^2 + 99\,360 - 49\,440\pi)\gamma + 30\pi - 120 \\
e_2 &= (-68\,896\pi^4 + 20\,570\,112\pi + 1156\,800\pi^3 - 21\,689\,856 - 7310\,880\pi^2)\gamma^3 + \\
&\quad (-27\,039\,744 - 4981\,248\pi^2 + 412\,416\pi^3 + 20\,086\,272\pi)\gamma^2 + \\
&\quad (140\,400 - 69\,840\pi + 8700\pi^2)\gamma + 42\pi - 168 \\
e_1 &= (486\,383\,616 + 1819\,136\pi^4 + 178\,569\,216\pi^2 - 29\,431\,296\pi^3 - 481\,406\,976\pi)\gamma^3 + \\
&\quad (-2864\,640\pi^2 + 11\,566\,080\pi - 15\,593\,472 + 236\,928\pi^3)\gamma^2 + \\
&\quad (6160\pi^2 + 99\,360 - 49\,440\pi)\gamma + 30\pi - 120 \\
e_0 &= (-3220\,224\pi^3 + 193\,664\pi^4 - 55\,240\,704\pi + 20\,035\,584\pi^2 + 56\,899\,584)\gamma^3 + \\
&\quad (1854\,720\pi - 2515\,968 - 456\,960\pi^2 + 37\,632\pi^3)\gamma^2 + \\
&\quad (29\,160 - 14\,520\pi + 1810\pi^2)\gamma - 36 + 9\pi \\
d_3 &= -16(1+R)^2(f_4R^4 + f_3R^3 + f_2R^2 + f_1R + f_0) \\
f_4 &= (3905\,280 - 233\,088\pi^3 + 14\,000\pi^4 - 3891\,456\pi + 1437\,264\pi^2)\gamma^3 + \\
&\quad (-16\,128\pi + 27\,648 + 3072\pi^2 - 192\pi^3)\gamma^2 + \\
&\quad (-3132 + 1548\pi - 192\pi^2)\gamma + 8 - 2\pi \\
f_3 &= (340\,032\pi^3 - 6027\,264 - 2066\,112\pi^2 - 21\,504\pi^4 + 5709\,312\pi)\gamma^3 + \\
&\quad (115\,968\pi^2 - 479\,232\pi + 663\,552 - 9408\pi^3)\gamma^2 + \\
&\quad (-622\pi^2 - 10\,152 + 5016\pi)\gamma - 5\pi + 20 \\
f_2 &= (-68\,896\pi^4 + 20\,570\,112\pi + 1156\,800\pi^3 - 21\,689\,856 - 7310\,880\pi^2)\gamma^3 + \\
&\quad (1714\,176 + 308\,736\pi^2 - 25\,344\pi^3 - 1257\,984\pi)\gamma^2 + \\
&\quad (-12\,312 + 6072\pi - 752\pi^2)\gamma - 6\pi + 24 \\
f_1 &= (-9234\,432 - 17\,792\pi^4 - 2600\,640\pi^2 + 358\,592\pi^3 + 8114\,688\pi)\gamma^3 + \\
&\quad (115\,968\pi^2 - 479\,232\pi + 663\,552 - 9408\pi^3)\gamma^2 + \\
&\quad (-622\pi^2 - 10\,152 + 5016\pi)\gamma - 5\pi + 20 \\
f_0 &= +(-225\,088\pi^3 + 15\,600\pi^4 - 2854\,656\pi + 1206\,864\pi^2 + 2522\,880)\gamma^3 + \\
&\quad (-16\,128\pi + 27\,648 + 3072\pi^2 - 192\pi^3)\gamma^2 + \\
&\quad (-3132 + 1548\pi - 192\pi^2)\gamma + 8 - 2\pi
\end{aligned}$$

$$d_2 = 2(1 + R)^2 (g_4 R^4 + g_3 R^3 + g_2 R^2 + g_1 R + g_0)$$

$$g_4 = (9372672 - 534528\pi^3 + 31552\pi^4 - 9206784\pi + 3349440\pi^2) \gamma^3 + (-152064 + 2656\pi^3 - 31200\pi^2 + 120384\pi) \gamma^2 + (-3456 + 1632\pi - 196\pi^2) \gamma + 36 - 9\pi$$

$$g_3 = (-1544448\pi^3 + 24551424 + 9416448\pi^2 + 93184\pi^4 - 25049088\pi) \gamma^3 + (-114432\pi^2 + 419328\pi - 497664 + 10176\pi^3) \gamma^2 + (-1192\pi^2 - 19872 + 9696\pi) \gamma - 12\pi + 48$$

$$g_2 = (133248\pi^4 - 25214976\pi - 1969920\pi^3 + 21731328 + 10696320\pi^2) \gamma^3 + (1838592 + 318336\pi^2 - 25728\pi^3 - 1321344\pi) \gamma^2 + (-12096 + 5760\pi - 696\pi^2) \gamma - 18\pi + 72$$

$$g_1 = (12607488 + 107008\pi^4 + 7425792\pi^2 - 1475328\pi^3 - 16091136\pi) \gamma^3 + (-114432\pi^2 + 419328\pi - 497664 + 10176\pi^3) \gamma^2 + (-1192\pi^2 - 19872 + 9696\pi) \gamma - 12\pi + 48$$

$$g_0 = (-515328\pi^3 + 35392\pi^4 - 6718464\pi + 2796480\pi^2 + 6054912) \gamma^3 + (113472\pi - 138240 - 30624\pi^2 + 2720\pi^3) \gamma^2 + (-3456 + 1632\pi - 196\pi^2) \gamma - 36 + 9\pi$$

$$d_1 = 2(1 + R)^2 (h_4 R^4 + h_3 R^3 + h_2 R^2 + h_1 R + h_0)$$

$$h_4 = (-57024\pi^3 + 3872\pi^4 - 746496\pi + 311328\pi^2 + 663552) \gamma^3 + (-13824 + 416\pi^3 - 4128\pi^2 + 13248\pi) \gamma^2 + (360\pi - 48\pi^2 - 648) \gamma + 3\pi - 12$$

$$h_3 = (148224\pi^3 - 3151872 - 1021824\pi^2 - 7552\pi^4 + 2985984\pi) \gamma^3 + (-216576\pi - 4800\pi^3 + 276480 + 56064\pi^2) \gamma^2 + (152\pi^2 - 1248\pi + 2592) \gamma$$

$$h_2 = (-25920\pi^4 + 5474304\pi + 395136\pi^3 - 4976640 - 2223936\pi^2) \gamma^3 + (-32640\pi^2 + 132480\pi + 2688\pi^3 - 179712) \gamma^2 + (720\pi - 96\pi^2 - 1296) \gamma + 6\pi - 24$$

$$h_1 = (-497664 - 10624\pi^4 - 579456\pi^2 + 132864\pi^3 + 995328\pi) \gamma^3 + (-216576\pi - 4800\pi^3 + 276480 + 56064\pi^2) \gamma^2 + (152\pi^2 - 1248\pi + 2592) \gamma$$

$$h_0 = (-57024\pi^3 + 3872\pi^4 - 746496\pi + 311328\pi^2 + 663552) \gamma^3 + (20160\pi + 352\pi^3 - 27648 - 4704\pi^2) \gamma^2 + (360\pi - 48\pi^2 - 648) \gamma + 3\pi - 12$$

$$\begin{aligned}
d_0 &= k_6 R^6 + k_5 R^5 + k_4 R^4 + k_3 R^3 + k_2 R^2 + k_1 R + k_0 \\
k_6 &= (-235\,872\pi^2 + 608\,256\pi - 2528\pi^4 - 580\,608 + 40\,128\pi^3) \gamma^3 + \\
&\quad (4272\pi^2 + 17\,280 - 400\pi^3 - 14\,976\pi) \gamma^2 + \\
&\quad (216 - 120\pi + 16\pi^2) \gamma - \pi + 4 \\
k_5 &= (-7744\pi^4 + 114\,048\pi^3 - 1327\,104 + 1492\,992\pi - 622\,656\pi^2) \gamma^3 + \\
&\quad (-32\pi^3 - 6912 + 3456\pi - 288\pi^2) \gamma^2 + \\
&\quad (-240\pi + 32\pi^2 + 432) \gamma \\
k_4 &= (-7456\pi^4 + 995\,328\pi - 746\,496 - 478\,368\pi^2 + 98\,880\pi^3) \gamma^3 + \\
&\quad (18\,432\pi - 24\,192 + 368\pi^3 - 4560\pi^2) \gamma^2 + \\
&\quad (-360\pi + 648 + 48\pi^2) \gamma + 12 - 3\pi \\
k_3 &= (552\,960\pi - 256\,896\pi^2 + 52\,480\pi^3 - 442\,368 - 3968\pi^4) \gamma^3 + \\
&\quad (-480\pi + 864 + 64\pi^2) \gamma \\
k_2 &= (-588\,960\pi^2 + 1492\,992\pi + 102\,720\pi^3 - 6688\pi^4 - 1410\,048) \gamma^3 + \\
&\quad (-4272\pi^2 + 14\,976\pi + 400\pi^3 - 17\,280) \gamma^2 + \\
&\quad (-360\pi + 648 + 48\pi^2) \gamma - 3\pi + 12 \\
k_1 &= (-7744\pi^4 + 114\,048\pi^3 - 1327\,104 + 1492\,992\pi - 622\,656\pi^2) \gamma^3 + \\
&\quad (288\pi^2 - 3456\pi + 32\pi^3 + 6912) \gamma^2 + \\
&\quad (-240\pi + 32\pi^2 + 432) \gamma \\
k_0 &= (38\,848\pi^3 + 442\,368\pi - 199\,008\pi^2 - 359\,424 - 2784\pi^4) \gamma^3 + \\
&\quad (-368\pi^3 + 4560\pi^2 - 18\,432\pi + 24\,192) \gamma^2 + \\
&\quad (216 - 120\pi + 16\pi^2) \gamma + 4 - \pi
\end{aligned}$$

References

- [1] M. di Bernardo, C.J. Budd, A.R. Champneys, P. Kowalczyk, *Piecewise-Smooth Dynamical Systems. Theory and Applications*. Series: Applied Mathematical Sciences, vol. 163. Springer, Berlin (2008).
- [2] A.C.J.Luo, *Singularity and Dynamics on Discontinuous Vector Fields*. Monograph Series on Nonlinear Science and Complexity, vol. 3. Elsevier, Amsterdam (2006).
- [3] J. Awrejcewicz, C.-H. Lamarque, *Bifurcation and Chaos in Nonsmooth Mechanical Systems*. World Scientific Series on Nonlinear Science: Series A, vol. 45. World Scientific Publishing, Singapore (2003).
- [4] A.F. Filippov, *Differential Equations with Discontinuous Right-Hand Sides*. Kluwer Academic, Dordrecht (1988).

- [5] W.J. Stronge, *Impact mechanics*. Cambridge University Press, Cambridge (2000).
- [6] A. Mehta (ed.), *Granular Matter: An Interdisciplinary Approach*. Springer, Berlin (1994).
- [7] C. Knudsen, R. Feldberg, H. True, Bifurcations and chaos in a model of a rolling wheel-set. *Philos. Trans. R. Soc. Lond. A* **338**, 455–469 (1992).
- [8] M. Wiercigroch, A.M. Krivtsov, J. Wojewoda, Vibrational energy transfer via modulated impacts for percussive drilling, *Journal of Theoretical and Applied Mechanics* **46**, 715–726 (2008).
- [9] J. Awrejcewicz, G. Kudra, G. Wasilewski, Experimental and numerical investigation of chaotic regions in the triple physical pendulum, *Nonlinear Dynamics* **50**, 755–766 (2007).
- [10] Holmes, P.J.: The dynamics of repeated impacts with a sinusoidally vibrating table. *J. Sound and Vibration* **84**, 173-189 (1982).
- [11] A.C.J. Luo, R.P.S. Han, The dynamics of a bouncing ball with a sinusoidally vibrating table revisited, *Nonlinear Dynamics* **10**, 1–18 (1996).
- [12] A.C.J. Luo, Y. Guo, Motion Switching and Chaos of a Particle in a Generalized Fermi-Acceleration Oscillator, *Mathematical Problems in Engineering*, vol. **2009**, Article ID 298906, 40 pages, 2009.
- [13] A.B. Nordmark, Existence of periodic orbits in grazing bifurcations of impacting mechanical oscillator, *Nonlinearity* **14**, 1517–1542 (2001).
- [14] S. Lenci, G. Rega, Periodic solutions and bifurcations in an impact inverted pendulum under impulsive excitation, *Chaos, Solitons and Fractals* **11**, 2453–2472 (2000).
- [15] A. Okniński, B. Radziszewski, Simple models of bouncing ball dynamics and their comparison, arXiv:1002.2448 [nlin.CD] (2010).
- [16] A. Okniński, B. Radziszewski, Dynamics of impacts with a table moving with piecewise constant velocity, *Nonlinear Dynamics* **58**, 515–523 (2009).
- [17] A. Okniński, B. Radziszewski, Chaotic dynamics in a simple bouncing ball model, *Acta Mech. Sinica* **27**, 130–134 (2011), arXiv:1002.2448 [nlin.CD] (2010).
- [18] A. Okniński, B. Radziszewski, Simple model of bouncing ball dynamics: displacement of the table assumed as quadratic function of time, *Nonlinear Dynamics* **67**, 1115–1122 (2012).
- [19] A. Okniński, B. Radziszewski, Simple model of bouncing ball dynamics. Displacement of the limiter assumed as a cubic function of time., *Differential Equations and Dynamical Systems* **21**, 165–171 (2013).

- [20] P. Pierański, Jumping particle model. Period doubling cascade in an experimental system, *J. Phys. (Paris)* **44**, 573–578 (1983).
- [21] N.B. Tuffiaro, T.M. Mello, Y.M. Choi, N.B. Albano, Period doubling boundaries of a bouncing ball, *J.Phys (Paris)* **47**, 1477–1482 (1986).
- [22] S. Celaschi, R.L. Zimmerman, Evolution of a two-parameter chaotic dynamics from universal attractors, *Phys. Lett.* **120A**, 447–451 (1987).
- [23] P. Pierański, R. Barberi, *Bouncing Ball Workbench*, OWN Poznań (1994).
- [24] B. Eichwald, M. Argentina, X. Noblin, F. Celestini, Dynamics of a ball bouncing on a vibrated elastic membrane, *Phys. Rev.* **E82**, 016203 (2010).
- [25] A. Okniński, B. Radziszewski, Grazing dynamics and dependence on initial conditions in certain systems with impacts, arXiv:0706.0257v2 [nlin.CD] (2007).
- [26] A.C.J.Luo, *Discontinuous Dynamical System on Time-varying Domains*. Series: Nonlinear Physical Science. Higher Education Press, Beijing and Springer, Dordrecht, Heidelberg, London, New York (2009).
- [27] E.I.Jury, *Inners and Stability of Dynamic Systems*. Wiley, New York (1974) [2nd edn., Krieger, Malabar, 1982].
- [28] S.G. Krantz, H.R. Parks, *The implicit function theorem: history, theory, and applications*. Birkhäuser, Boston (2002).
- [29] H.O. Peitgen, H. Jürgens, and D. Saupe, *Fractals for the Classroom. Part Two: Complex Systems and Mandelbrot Set.*, Springer, New York (1992).
- [30] S. Giusepponi, F. Marchesoni, The chattering dynamics of an ideal bouncing ball, *Europhysics Letters* **64**, 36 (2003).
- [31] S. Giusepponi, F. Marchesoni, M. Borromeo, Randomness in the bouncing ball dynamics, *Physica A* **351**, 142–158 (2005).